Fusion Engineering and Design 100 (2015) 81–86

Contents lists available at ScienceDirect

Fusion Engineering and Design

journal homepage: www.elsevier.com/locate/fusengdes

Nuclear data for fusion: Validation of typical pre-processing methods for radiation transport calculations

T. Hutton[a,b,*], J.C. Sublet[b], L. Morgan[b], T.W. Leadbeater[a]

[a] School of Physics and Astronomy, University of Birmingham, B15 2TT, UK
[b] Culham Centre for Fusion Energy, OX14 3DB, UK

HIGHLIGHTS

- We quantify the effect of processing nuclear data from ENDF to ACE format.
- We consider the differences between fission and fusion angular distributions.
- C-nat(n,el) at 2.0 MeV has a 0.6% deviation between original and processed data.
- Fe-56(n,el) at 14.1 MeV has a 11.0% deviation between original and processed data.
- Processed data do not accurately depict ENDF distributions for fusion energies.

ARTICLE INFO

Article history:
Received 27 February 2015
Accepted 17 April 2015
Available online 21 May 2015

ABSTRACT

Nuclear data form the basis of the radiation transport codes used to design and simulate the behaviour of nuclear facilities, such as the ITER and DEMO fusion reactors. Typically these data and codes are biased towards fission and high-energy physics applications yet are still applied to fusion problems. With increasing interest in fusion applications, the lack of fusion specific codes and relevant data libraries is becoming increasingly apparent. Industry standard radiation transport codes require pre-processing of the evaluated data libraries prior to use in simulation. Historically these methods focus on speed of simulation at the cost of accurate data representation. For legacy applications this has not been a major concern, but current fusion needs differ significantly. Pre-processing reconstructs the differential and double differential interaction cross sections with a coarse binned structure, or more recently as a tabulated cumulative distribution function. This work looks at the validity of applying these processing methods to data used in fusion specific calculations in comparison to fission. The relative effects of applying this pre-processing mechanism, to both fission and fusion relevant reaction channels are demonstrated, and as such the poor representation of these distributions for the fusion energy regime. For the ^{nat}C(n,el) reaction at 2.0 MeV, the binned differential cross section deviates from the original data by 0.6% on average. For the ^{56}Fe(n,el) reaction at 14.1 MeV, the deviation increases to 11.0%. We show how this discrepancy propagates through to varying levels of simulation complexity. Simulations were run with Turnip-MC and the ENDF-B/VII.1 library in an effort to define a new systematic error for this range of applications. Alternative representations of differential and double differential distributions are explored in addition to their impact on computational efficiency and relevant simulation results.

© 2015 The Authors. Published by Elsevier B.V. This is an open access article under the CC BY license (http://creativecommons.org/licenses/by/4.0/).

1. Introduction

The Monte Carlo method has been used for many years to simulate the transport of uncharged and charged radiation throughout fission reactors and other nuclear facilities, and as such, there are multiple codes designed for this purpose. The progression towards nuclear fusion as a commercially viable power source demands a closer look to be taken at the applicability of the currently available legacy codes and data to such purposes. The neutron fluxes predicted in ITER and future fusion reactors will be far higher than that seen in any current devices in civil nuclear technology. The interaction of the 14.1 MeV neutrons from D-T fusion with the reactor components cause radiation damage, activation and heating. These reactions must be accurately predicted to determine the shielding and lifetime requirements as with any other reactor. For D-T fusion

* Corresponding author at: School of Physics and Astronomy, University of Birmingham, B15 2TT, UK. Tel.: +44 1214144668.
E-mail address: txh739@bham.ac.uk (T. Hutton).

http://dx.doi.org/10.1016/j.fusengdes.2015.04.045
0920-3796/© 2015 The Authors. Published by Elsevier B.V. This is an open access article under the CC BY license (http://creativecommons.org/licenses/by/4.0/).

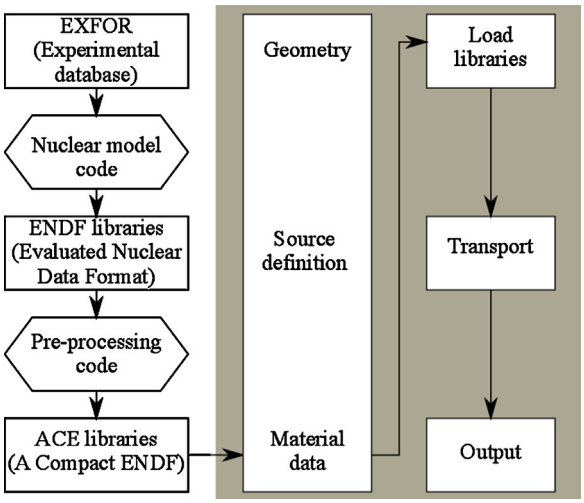

Fig. 1. Block diagram to show the flow of nuclear data from experimental measurements stored in the EXFOR [4] database through to use in radiation transport codes. The experimental data are selected by evaluators to use within nuclear model codes, to construct continuous data libraries in the ENDF format. For use in radiation transport codes such as MCNP or Serpent, the data must be further processed via pre-processing codes such as NJOY, into the ACE format. A detailed description of this can be found in [5]. The shaded region shows the simplified use of these data within a generic radiation transport input file through to an output value from the code that can be used to calculate relevant quantities.

devices in particular, the breeding of tritium as a fuel within the reactor is necessary to ensure self-sufficiency. The relevant reaction channels are induced by neutrons and so the associated data must be accurate to determine the location and quantity of the tritium for extraction. This is just one example of many of the important neutron interactions within a fusion device. The neutronics modelling of these devices must be of an exceptionally high quality to ensure the safe operation of financially viable fusion reactors, in particular with respect to shielding, design tolerances and breeder blanket optimisation. The current practice for modelling these devices consists of using the available radiation transport codes, designed for an alternative purpose, with fusion specific nuclear data. This is not ideal as the requirements for fusion modelling differ from those for fission. Furthermore, the current fusion data libraries are incomplete; thus implying a need for future experimental studies to populate these libraries. In the longer term, a specialised set of codes and data would be created for fusion neutronics, but for current facilities and experiments it is not feasible to wait for this to be implemented. This study considers how the processing and neutronics codes handle nuclear data within the current modelling methods; in addition to exploring alternatives that could be implemented within future code developments for fusion neutronics.

Radiation transport codes are only ever as accurate as the model supplied to them. This includes the use of materials and their corresponding interaction data. These data start as experimental results produced by multiple facilities worldwide, they undergo a series of processes before they are able to be used within the radiation transport codes. The process from experimental data to libraries suitable for use in neutronics modelling is shown in Fig. 1. In this instance we focus on ENDF[1] data processed by NJOY [1] to be used within the radiation transport code, MCNP [2]. This combination of the NJOY pre-processing code and MCNP radiation transport code is considered to be the industry standard for typical simulations. The initial phases of pre-processing include the reconstruction of interaction cross sections with resonances to interpolated data points on a fine energy grid. The differential and double differential cross sections[2] undergo a different type of processing. NJOY allows two different ways of dealing with these distributions; a legacy method that is fast to sample as part of the Monte Carlo (MC) approach and minimises data requirements, or a newer method that tends to better represent the data in comparison [3], though this has never strictly been quantified. The cost of this is a longer sampling time and larger data file. A major consideration when running MC simulations of ITER scale is computational efficiency. Not only are huge numbers of individual histories required to achieve the necessary statistical convergence, but all material data required for the simulation is loaded into physical memory. From here the data are accessed, so the amount of available memory is an additional limiting factor for these simulations. For this reason we will be looking at the applicability of the legacy method of data processing to fusion data, to determine if the loss in data accuracy outweighs the need for computational efficiency.

When the MC method is applied to neutron transport, many histories are run and these each undergo a series of interactions to simulate the average behaviour of neutrons within the system. Examples of how this average behaviour is used are:

- to determine the energy dependent neutron flux incident on a breeder blanket, which in turn leads to calculations for tritium self-sufficiency;
- to check if any streaming occurs from the vacuum vessel and hence determine shielding requirements in these areas;
- to calculate the corresponding activation calculation of materials post irradiation.

Each interaction within the history is determined by the random sampling of the nuclear data. Of particular interest here is the sampling of the differential and double differential cross section distributions to determine the exit energy and angles of radiative particles after each interaction. The MC process used by MCNP is described by the block diagram in Fig. 2, with each sampling stage indicated.

The original method for processing the differential and double differential cross section distributions is to represent them with 32 equal probability channels. This particular format is specific to the ACE files used in MCNP, though many other codes use an equal probability structure in a similar fashion with differing numbers of channels. The downfall of using this representation is the loss of features or information within the range of the reaction distribution. For fission relevant reactions, this loss of information is less noticeable as these reactions tend to be more isotropic than those expected for fusion reactors. One example of this can be seen in Fig. 3. The reaction channels shown here are for angular distributions of elastically scattered neutrons from ^{nat}C at 2.0 MeV, i.e. a fission relevant reaction channel, and from ^{56}Fe at 14.1 MeV, a fusion relevant reaction channel. In the fission specific case, the function is more isotropic in scattering cosine than the fusion specific case, in the sense that there is little or no forward bias and no major features. This is reinforced when one considers the complexity of the distributions, the ^{nat}C distribution is described by a 4th order polynomial, but the ^{56}Fe distribution requires a 12th order polynomial as determined by the evaluators and nuclear models. This is fairly typical for the majority of fission and fusion channels, though in some cases the polynomials can be much more complex. When the equal probability format is considered for the fusion specific channel, much of the fine detail in the lower probability region is lost. For the fission specific case, the bins are more evenly

[1] For a list of acronyms used here and their definitions, see Appendix A

[2] Distributions for reaction products with respect to angle and/or energy

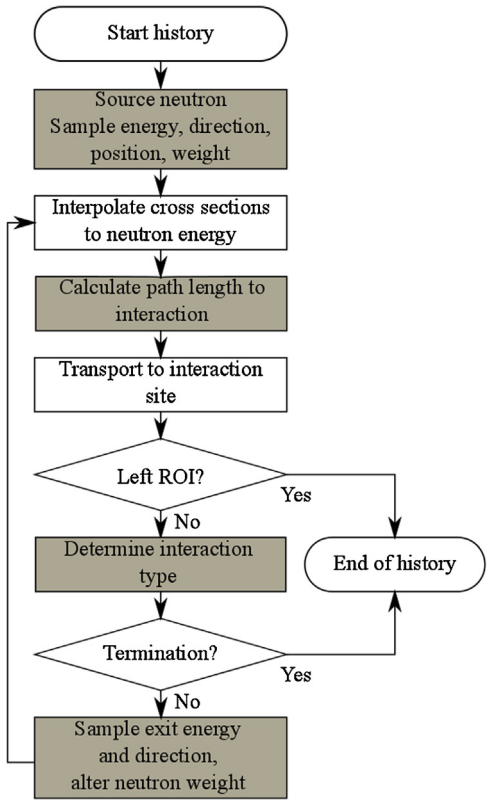

Fig. 2. Flow diagram to show the simplified transport process for a single neutron history, in radiation transport code MCNP. Stages where sampling is required are indicated by the shaded areas. The area of interest for this paper is the sampling of exit direction and energy.

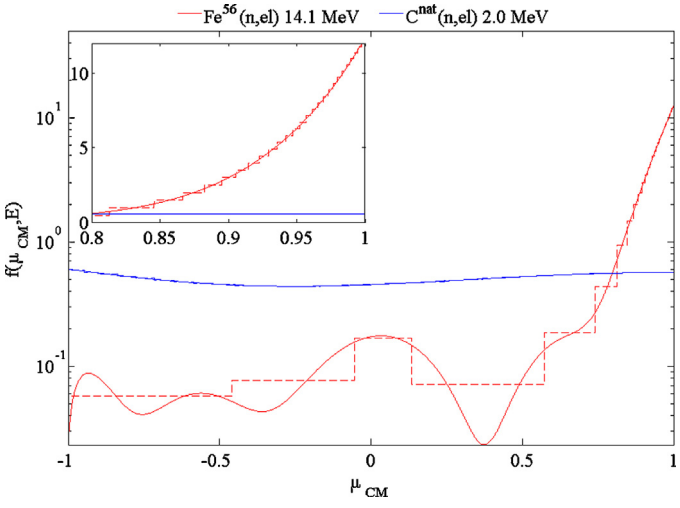

Fig. 3. Normalised probability distribution functions $f(\mu, E)$ for the elastic scatter of neutrons from ^{56}Fe at 14.1 MeV (red) and ^{nat}C at 2.0 MeV (blue). The solid lines represent the polynomial distributions as taken from the ENDF/B-VII.1 files and the dashed lines represent the processed equivalent. The abscissa represents the cosine of the scattering angle, μ, for a single scatter in the centre of mass (CM) frame, and the ordinate represents the normalised probability distribution function for a neutron at energy, E, scattering into μ. The inset shows the forward scattering section of the distributions on a linear scale to highlight the high level of anisotropy for the ^{56}Fe reaction and the effect of applying the histogram over areas with a high rate of change. (For interpretation of the references to color in this figure legend, the reader is referred to the web version of this article.)

Table 1
List of variables used in Eqs. (1)–(3) with associated definitions.

Variable	Description
μ	Scattering cosine in CM frame (unit cosine^{-1})
E	Neutron energy (eV)
$f(\mu, E)$	Differential probability distribution for incident E and exit μ
P_l	Legendre polynomial of order l
a_l	Coefficient l as given in ENDF file
NL	Maximum order of Legendre polynomial
$P(\mu, E)$	Probability distribution function used for sampling in MC
$\sigma(\mu, E)$	Differential cross section ($b \cdot sr^{-1}$)[a]
$\sigma_s(E)$	Elastic scattering cross section (b)

[a] This can also be written as $\frac{d\sigma_s(E)}{d\Omega}$, where $d\Omega$ is the solid angle subtended by $\sin\theta \cdot d\theta \cdot d\phi$.

distributed over the range in μ and will be shown to better represent the function.

2. Approach

In order to determine the effect of the processing methods used on final simulation results, it is necessary to first consider the nuclear data as given in the ENDF file. While these data form is not necessarily exact with respect to the original experimental data, it is taken as the reference for the most accurate input to the transport codes and is used here to define a standard by which the pre-processing methods can be compared against. The ENDF/B-VII.1 library was used in this work. This was parsed to extract the relevant information for each isotope and energy. For the elastic scatter of neutrons from ^{56}Fe [6] and ^{nat}C [7], the associated reaction cross sections were extracted, along with the differential data which correspond to the polar angular distribution of the scatter. For the energies considered data were given in terms of Legendre coefficients. Eq. (1) shows how the normalised probability distribution, $f(\mu, E)$ is determined at a certain energy with respect to the scattering cosine in the centre of mass frame (see Table 1 for variable definitions). $f(\mu, E)$ is calculated from the coefficients $a_l(E)$ as given in the ENDF file for each energy in combination with the Legendre polynomials, $P_l(\mu)$. This angular distribution is normalised, so that the integral between the limits of $-1 \leq \mu \leq 1$ is equal to 1. To obtain the true differential cross section, $\sigma(\mu, E)$, the normalised angular distribution must be multiplied by the reaction channel cross section, $\sigma(E)$ as extracted from elsewhere within the file.

$$f(\mu, E) = \sum_{l=0}^{NL} \frac{2l+1}{2} a_l(E) P_l(\mu) \tag{1}$$

$$P(\mu, E) = \int_{-1}^{\mu} f(\mu, E) d\mu \tag{2}$$

$$\sigma(\mu, E) = \frac{\sigma_s(E)}{2\pi f(\mu, E)} \tag{3}$$

The normalised angular probability distributions were reconstructed at the relevant energies into their exact functional forms,[3] and then processed into the 32 equal probability bin format as used in the MCNP data files. This structure was calculated using Eq. (4), where k is the bin number and N is the total number of bins, in this instance $N = 32$. To find the limits of μ for each bin, the integral was

[3] This representation cannot currently be used by MCNP or other radiation transport codes, but may be implemented in future developments.

evaluated exactly with numerical Gaussian quadrature to the same precision as the input data.

$$\int_{-1}^{\mu_k} f(\mu, E)d\mu = \frac{k}{N} \tag{4}$$

The processed data form was compared to the exact functional form for each reaction channel with three levels of analysis.

1. Point-wise analysis
2. Simple statistical analysis using Turnip-MC[4]
3. Statistical analysis with transport using Turnip-MC

Point-wise analysis requires both distributions to be evaluated on a fine μ grid of 10^5 equally spaced samples, where the differences between them are considered in the centre of mass frame. The second level employs the use of a reaction channel Monte Carlo code, Turnip-MC. This stage simulates large numbers of statistically identical events without the complexities of geometry, material compositions, etc. as would be present in traditional radiation transport codes. This allows a closer look at how distributions are sampled and how any deviations here might propagate through to observables. In a similar fashion multiple events can be studied along with their resulting probability distribution functions. The final stage of analysis here allows for the full transport of particles, whilst still only allowing a single reaction channel. This includes full scattering kinematics and the resulting histories were histogrammed with respect to exit angle and energy across a spherical surface.

To quantify the differences between exact and processed data formats two main metrics are used; the maximum difference, Δ, and the coefficient of variation, C_v. The maximum difference, as given by Eq. (5), provides information on any narrow or peaked features that would otherwise be lost in averages and retains the nature of the difference, thus quantifying over or underestimation. This tends to be the standard nuclear data method for comparing two data sets [8, p. 300]. The coefficient of variation, as given in Eq. (7), is derived from the statistical mean of the deviations. The arithmetic mean provides no usable information concerning the differences, as by definition this is zero. The root mean square deviation provides information on how far, on average, the difference deviates from zero as shown in Eq. (6), by normalising we get the coefficient of variation. This provides a measure of the extent of variability with respect to the mean of the distributions, though the nature of the deviations is lost. These two metrics have been used to provide a consistent measure of variability over each level of analysis.

$$\Delta = \max_{-1\le\mu\le1} |f(\mu) - h(\mu)| \tag{5}$$

$$RMSD = \sqrt{\frac{1}{n}\sum_{i=0}^{n}(f(\mu_i) - h(\mu_i))^2} \tag{6}$$

$$C_v = \frac{RMSD}{\overline{h(\mu)}} \tag{7}$$

2.1. Point-wise results

Both functions and reaction channels were calculated on a fine scattering cosine grid, with the number of points determined by a simple sensitivity study to ensure convergence. Fig. 4 shows the results of the difference measurements for the ^{56}Fe and the ^{nat}C (n,el) reaction channels over the entire range in μ for the given energies. From this figure it is clear to see that for this fusion reaction the low probability events are poorly represented, but the main contributing factor for the differences corresponds to the forward peaked section. Table 2 presents the metrics as described in Section 2, the maximum difference for the considered ^{56}Fe reaction channel is an order of magnitude greater than that for ^{nat}C. Both maximum differences are negative, corresponding to an underestimate of a feature by the histogram. It is worth noting that the mean difference is zero; the processing of the raw data introduces an error on a point-by-point basis, but does not introduce a systematic error over the entire range of the distribution. This point-by-point deviation shows a loss of features within each channel. For the ^{56}Fe reaction channel the residuals vary by 11.0% on average from the mean, though on a continuous basis (see Fig. 4) this can range up to 52.4%. For the ^{nat}C reaction, the coefficient of variation is two orders of magnitude lower at 0.6%, ranging up to 2.4%. Comparing the fission and fusion reaction channels, the histogram format is a better representation for more isotropic events considered. The high level of anisotropy for the fusion reaction channel not only makes it difficult to retain detail in the back scattering region, but is mis-represented in areas with a large rate of change.

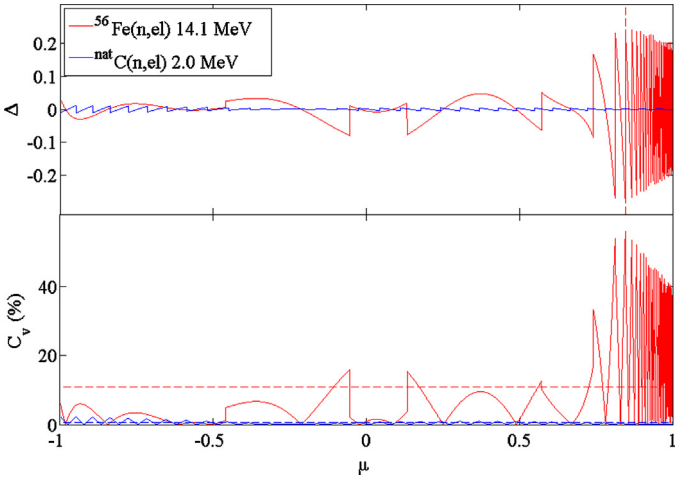

Fig. 4. Top: Difference between the functional and histogrammed distributions, with the point of maximum difference marked with dashed lines. Bottom: Coefficients of variation for the histogram data with respect to the functional form, with overall values marked with dashed lines. Refer to Fig. 3 for original distributions.

2.2. Statistical results

Turnip-MC was passed both the functional and histogrammed data for each reaction channel, with the histogram sampled accordingly and the functional form solved with an iterative search. Fig. 5 shows the distributions for 1, 2 and 3 scatters for the ^{56}Fe reaction channel with functional and histogrammed data. For comparison, the equivalent simulation results for the ^{nat}C reaction channel can be seen in Fig. 6. For 1 through to 10 scatters, the coefficient of vari-

Table 2
Calculated values for maximum difference and coefficient of variation from analytical comparison of histogrammed data format with respect to exact functional form for the ^{56}Fe and ^{nat}C reaction channels.

	Δ	C_v(%)
^{nat}C(n,el) 2.0 MeV	−0.012	0.6
^{56}Fe(n,el) 14.1 MeV	−0.265	11.0

[4] In-house Monte Carlo code for nuclear data analysis developed by T.W. Leadbeater, T. Hutton, Nuclear Data Group, University of Birmingham, UK

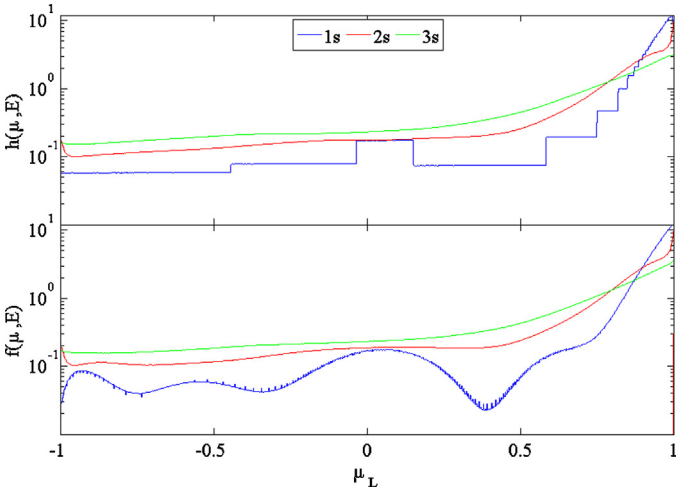

Fig. 5. Turnip-MC results for multiple scatter showing continuous distributions for the ^{56}Fe(n,el) reaction channel at 14.1 MeV in the lab frame. Top: Normalised probability distributions for exit scattering cosine, μ for 1, 2 and 3 scatters with histogram data. Bottom: As above, with exact functional data.

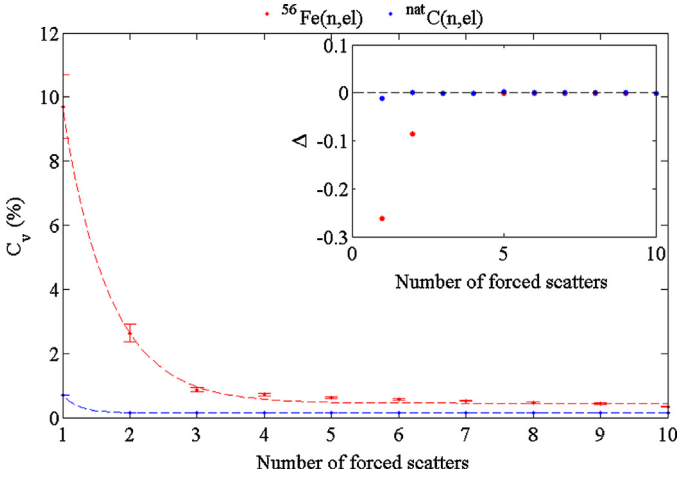

Fig. 7. Calculated coefficient of variation with number of forced scatters with Turnip-MC. Dashed lines correspond to an exponential fit to the form of $a \cdot \exp(-b \cdot x) + c$. Inset: Maximum difference for 1–10 forced elastic scatters in ^{56}Fe (red) and ^{nat}C (blue). (For interpretation of the references to color in this figure legend, the reader is referred to the web version of this article.)

ation and maximum difference were calculated. Fig. 7 shows how these metrics behave when propagated through multiple events. For both the ^{56}Fe and ^{nat}C channels considered here, there is an exponential fall off to a baseline of less than 1.0%. For the ^{56}Fe channel, the C_v does not drop below 1.0% until after three scatters. The maximum allowable statistical error for MCNP calculations is 10.0% [9, p. 2.116], so for the ^{nat}C reaction channel considered, the associated processing error is below this for any number of events. For the ^{56}Fe reaction channel, the average deviation is above this until the second scatter.

2.3. Statistical results with transport

Turnip-MC was run with histories originating at the centre of a unit-density sphere as a directional beam with an initial energy of 14.1 MeV or 2.0 MeV respectively for the ^{56}Fe and ^{nat}C reactions. For each reaction channel at the specific energy, the path length to the next interaction was determined by sampling of the scattering cross section, σ_s. The average number of scatters is dependent on the mean free path of the neutron, and approximately proportional to the square of the sphere radius. The coefficient of variation for the average number of scatters behaves in the same manner as with forced scatters (Fig. 7) for the two materials at relevant energies. With conventional transport and scattering kinematics, the variation of the processed and unprocessed distributions drops exponentially, as previously seen, to a baseline below the required MCNP error. This suggests that for a pure scatterer, if the material thickness is much greater than the mean free path of the neutron, then the errors are dominated by statistics. On the other hand, if we have a material with a thickness of the order of one mean free path, or lower, the observed error would be dominated by the processing.

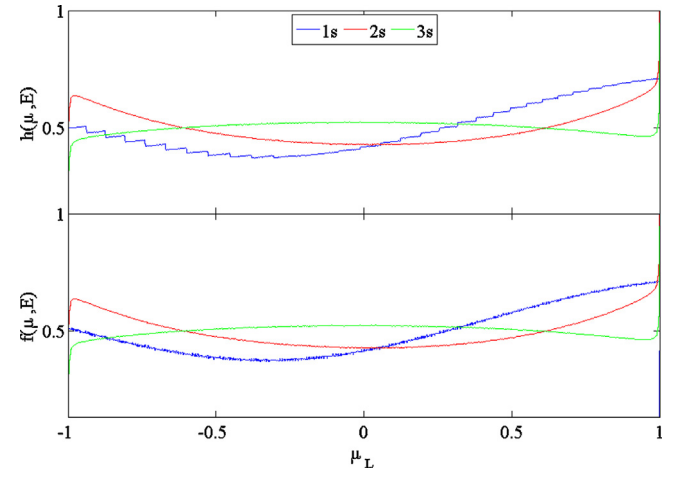

Fig. 6. Turnip-MC results for multiple scatter to show continuous distributions for the ^{nat}C(n,el) reaction channel at 2.0 MeV in the lab frame. Top: Normalised probability distributions for exit scattering cosine, μ for 1, 2 and 3 scatters with histogram data. Bottom: As above with exact functional distributions.

3. Conclusions

Based on the reaction channels considered in the study, the 32 binned format is not a suitable structure for reaction channels with a high level of anisotropy. The average deviation of the fusion type reaction channel, ^{56}Fe(n,el) at 14.1 MeV was 11.0%. For ^{nat}C(n,el) at 2.0 MeV reaction channel the deviation is much lower at only 0.6%. These deviations would be most noticeable in thin target experiments, or for rare events. In these instances, the processing error would dominate the statistical error calculations. The low probability regions are described poorly with the 32 equiprobable bin format, this means that we gain little or no information about them. Regions with a high rate of change are mis-represented by the histogram format. However, if we consider how this might propagate through to large numbers of events, such as in a bulk shielding experiment, the error introduced by the processing of the original data drops below the statistical tolerance of most Monte Carlo radiation transport codes. It is worth noting that elastic scattering is the simplest distribution to consider. Within a full-scale reactor simulation, many other reactions occur and, in comparison to the elastic distributions, are much more complex in their structure. It is expected that the more complex the distribution, the greater the observed effect from processing the data. In addition to this we see mixing of isotopes to construct the required materials and have much more complex geometries than the simple sphere considered here. By introducing these additional complexities one would expect to see the effect of these deviations to become more prominent.

Acknowledgements

This work is supported by Culham Centre for Fusion Energy, UK, the University of Birmingham, UK and the Engineering and Physical Sciences Research Council.

Appendix A. Acronym definitions

Acronym	Definition
ACE	A Compact ENDF
ENDF	Evaluated Nuclear Data Format
EXFOR	EXchange FORmat
ITER	International Thermonuclear Experimental Reactor
MCNP	Monte Carlo N-Particle

References

[1] R.E. MacFarlane, D.W. Muir, R.M. Boicourt, A.C. Kahler, The NJOY Nuclear Data Processing System, Version 2012, Los Alamos National Laboratory, 2013.
[2] J.F. Briesmeister, MCNP: A General Monte Carlo N-Particle Transport Code, Los Alamos National Laboratory, 1993.
[3] R.E. MacFarlane, A.C. Kahler, Methods for processing ENDF/B-VII with NJOY, Nucl. Data Sheets 111 (12) (2010) 2781, Nuclear Reaction Data.
[4] N. Otuka, E. Dupont, V. Semkova, B. Pritychenko, A.I. Blokhin, M. Aikawa, et al., Towards a more complete and accurate experimental nuclear reaction data library (EXFOR): international collaboration between nuclear reaction data centres (NRDC), Nucl. Data Sheets 120 (2014) 272–276.
[5] R.E. MacFarlane, A.C. Kahler, Methods for processing ENDF/B-VII with NJOY, Nucl. Data Sheets 111 (12) (2010) 2739–2890, Nuclear Reaction Data.
[6] M.B. Chadwick, P.G. Young, C.Y. Fu, ENDF/B-VII.1 MAT 2631, 1996, September.
[7] M.B. Chadwick, P.G. Young, C.Y. Fu, ENDF/B-VII.1 MAT 600, 1996, June.
[8] D.G. Cacuci, Handbook of Nuclear Engineering: Nuclear Engineering Fundamentals, Springer, 2010.
[9] X-5 Monte Carlo Team, MCNP: A General Monte Carlo N-Particle Transport Code, Version 5, Los Alamos National Laboratory, 2003.